Electrochemical and Solid-State Letters, **14** (7) B74-B76 (2011)
1099-0062/2011/14(7)/B74/3/$28.00 © The Electrochemical Society

Effect of ZnCdSe/ZnSe Core/Shell Quantum Dots on the Efficiency of Organic Photovoltaic Cells

Kyoung Soon Choi,[a] Yensil Park,[a] Jae Soo Yoo,[a,*] Soo Young Kim,[a,z] Heesun Yang,[b] Gwan Ho Jung,[c] and Jong-Lam Lee[c,*]

[a]*School of Chemical Engineering and Materials Science, Chung-Ang University, Dongjak-gu, Seoul 156-756, Korea*
[b]*Department of Materials Science and Engineering, Hongik University, Seoul 121-791, Korea*
[c]*Department of Materials Science and Engineering, Pohang University of Science and Technology, Pohang, Kyungbuk 790-784, Korea*

We report on the effect of ZnCdSe/ZnSe core/shell quantum dots (QDs) on the efficiency of organic photovoltaic (OPV) cells. The QDs were deposited on the back side of indium tin oxide (ITO)/glass substrates by spin coating with poly(methyl methacrylate). The short circuit current and power conversion efficiency of the OPV cells on the ITO/glass/QDs + PMMA substrate (8.5 mA/cm^2 and 3.2%) are lower than those of the control device on the ITO/glass substrate (9.0 mA/cm^2 and 3.4%), due to the low transmittance of the QDs + PMMA and discordance between the emission peak of the QDs and absorption peak of the active area in the OPV cells. It is anticipated that the usage of QDs whose emission peak is coincident with the absorption peak of the active area would improve the performance of the OPV cells.
 [DOI: 10.1149/1.3589246]

Manuscript submitted February 7, 2011; revised manuscript received March 22, 2011. Published April 29, 2011.

Organic photovoltaic (OPV) cells composed of solution-processed materials have emerged as one of the promising alternatives to silicon based solar cells, due to their many potential benefits, particularly for low-cost, large-area, and mechanically flexible substrates, as well as the possibility of using roll-to-roll fabrication processes.[1] OPV cells were fabricated with an active layer composed of a blend of regio-regular poly(3-hexylthiophene) (P3HT) as an electron donor and the fullerene derivative [6,6]-phenyl-C61 butyric acid methyl ester (PCBM) as an electron acceptor, and found to have a solar conversion efficiency greater than 6.5%.[2] However, this value is still lower than that of silicon based solar cells or dye-sensitized solar cells (DSSCs), so that many methods have been investigated. One of the methods involves colloidal semiconductor quantum dots (QDs) by making use of their novel optical and electrical properties resulting from their three-dimensional confinement. By combining different-sized QDs on one solar cell, researchers can create solar cells that absorb more light and, thereby, deliver power at greater efficiencies compared with solar cells made of bulk semiconductors. In the field of DSSCs, QDs made of CdS, PbS, PbSe, CdSe, InAs, or InP were assembled on the surface of TiO_2, and found to transfer electrons to the conduction band of TiO_2 upon visible light irradiation.[3–8] In the field of OPV cells, QDs made of CdS, CdSe, or PbS blended with an active layer were found to act as an electron acceptor with efficient charge generation and charge transport.[9–11] However, their device efficiency is reported to be very poor compared to that of OPV cells using PCBM as an electron acceptor.

ZnSe is a direct-band-gap semiconductor with a bulk band gap of 2.8 eV (below ca. 443 nm) and CdSe has a smaller band gap of 1.7 eV (below ca. 730 nm).[12,13] Therefore, ZnCdSe/ZnSe core/shell QDs can be classified as Type-I. In this kind of core/shell heterostructured QDs, the valence band in the core is higher than that in the shell, but the conduction band in the core is lower than that in the shell. It is reported that Type-I QD energy alignments produce a quantum well usually favoring exciton recombination and luminescence rather than dissociation.[14] As a result, QDs can be used to increase the emission efficiency at specific wavelength. If the wavelength of emitted light from QDs matches with absorption wavelength of active layer in OPV cells, it is expected that efficiency of the OPV cells will be enhanced.

In this letter, poly(methyl methacrylate) (PMMA) embedded with ZnCdSe/ZnSe core/shell QDs (QDs + PMMA) was used to enhance the absorbance of light and, thereby, deliver power at greater efficiencies. In order to attach ZnCdSe/ZnSe QDs on the opposite side of an indium tin oxide (ITO)/glass substrate, PMMA layer was used as supporting materials. The active layer of the OPV cells was composed of a blend of P3HT and PCBM. Thus, the QDs + PMMA would increase the light intensity so that more light will be absorbed to the OPV cells, thereby enhancing the efficiency of the OPV cells. Therefore, the effects of the QDs + PMMA on the performance of the OPV cells are discussed.

In a typical synthesis of the ZnCdSe quantum dots (QDs), 0.572 mmol of ZnO, 0.143 mmol of CdO, 1 ml of oleic acid, and 10 ml of 1-octadecene were placed in a three-neck reaction flask. The mixture was heated to 170°C during degassing. The mixture flask was then purged with argon and its temperature was raised to 310°C. At this temperature, 1 ml of oleylamine was rapidly injected first into the above hot mixture and then a Se solution containing 1.93 mmol of Se powder in 1 ml of trioctylphosphine was swiftly injected. The reaction mixture was maintained at 310°C for 20 min for the growth of the QDs. The surface of the ZnCdSe core QDs was subsequently coated with a ZnSe shell. A Zn stock solution was prepared by dissolving zinc acetate dehydrate (2.86 mmol) in a mixture of oleic acid (2 ml), oleylamine (2 ml) and 1-octadecene (1 ml) at 150°C and a Se stock solution was prepared by dissolving Se (7.72 mmol) in 4 ml of trioctylphosphine at the same temperature. For the coating of the ZnSe shell, the crude solution of the ZnCdSe core QDs was cooled to 190°C and the Se stock solution was injected into it first, followed by the dropwise addition of the Zn stock solution using a syringe pump. Then, the mixture was kept at 190°C for 20 min to complete the growth of the ZnSe shells. The ZnCdSe/ZnSe QDs were washed three times with a combined hexane/methanol solvent, and then dispersed in chlorobenzene.

A sol composed of 1 or 2 g of PMMA in 5 ml of chloroform was prepared and mixed with 2 ml of the QDs in chlorobenzene. Glass coated with ITO (150 nm thick, ~20 Ω/sq) was used as the starting substrate. The sol was coated on the back side of the ITO/glass substrate at a rate of 1000 rpm for 20 s. For use as a reference, an ITO/glass substrate without QDs + PMMA films was also prepared. Active blend films were fabricated between a transparent ITO anode and a reflective cathode. The ITO surface was cleaned using an O_2 plasma for 1 min under a pressure of 100 mTorr with a power of 150 W prior to device fabrication. After the O_2 plasma treatment, the substrates were transferred to an N_2-filled glove box. Poly(3,4-ethylenedioxythiophene):poly(styrene-sulfonate) (PEDOT:PSS) in OPV cells with P3HT:PCBM was spin-coated as a hole extraction layer. P3HT was first dissolved in 1,2-dichlorobenzene to make a 20 mg/ml solution, followed by blending with PCBM at a weight ratio of 1:1. The blend was stirred for ~14 h in a glove box before being spin-coated on top of the ITO anode. The thickness of the active layer was measured to be ~200 nm by a surface profiler. The

* Electrochemical Society Active Member.
z E-mail: sooyoungkim@cau.ac.kr

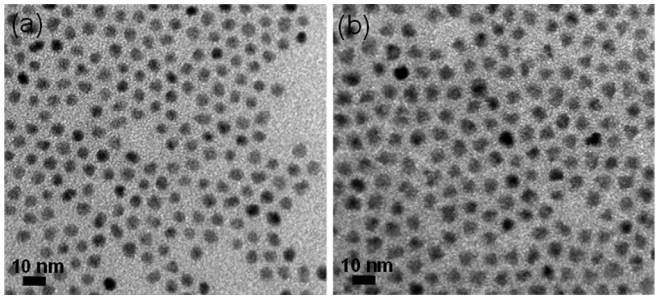

Figure 1. TEM images of (a) ZnCdSe core and (b) ZnCdSe/ZnSe core/shell QDs with average diameters of ∼5.5 and ∼7.5 nm, respectively.

devices were annealed on a hot plate in a glove box at 130°C for 10 min. The cathode were fabricated by depositing LiF (ca. 1 nm) and Al (ca. 100 nm) at a base pressure of 2×10^{-6} Torr. The active device area was ca. 0.04 cm^2. The current density-voltage (*J–V*) curves were measured under air ambient with glass encapsulation using a Keithley 2400 source measurement unit. The photocurrent was measured under AM1.5G 100 $mWcm^{-2}$ illumination. The maximum power conversion efficiency (PCE) for conversion of solar radiation to electrical power was calculated by $\frac{V_{oc} \times J_{sc} \times FF}{P_{in}(=100 mW/cm^{-2})} \times 100$, where V_{oc} is open circuit voltage, J_{sc} is short circuit current density, FF is fill factor, and P_{in} is the illuminated power.

The absorption characteristics of the QDs were measured by UV-visible absorption spectroscopy (Shimadzu, UV-2450). The photoluminescence (PL) spectra of the ZnCdSe/ZnSe QDs were collected by a spectrofluorometer (Jobin Yvon Inc., Fluorolog 3) equipped with a 450 W Xe lamp. The PL quantum yield of a diluted solution of the QDs with an optical density of ∼0.05 was calculated by comparing their integrated emission with that from a Rhodamine 6G standard solution. A JEOL 200 CX transmission electron microscopy (TEM) operating at an accelerating voltage of 200 kV was used to measure the size of the QDs.

To generate highly luminescent QDs by their effective surface passivation, the ZnCdSe core QDs were overcoated with a ZnSe shell having a higher band gap. As can be seen in the TEM images of the ZnCdSe core and ZnCdSe/ZnSe core/shell QDs (Figs. 1a and 1b, respectively), the average diameters of the core and core/shell QDs were measured to be ∼5.5 and ∼7.5 nm, respectively, which indicates that the shell thickness is ∼1 nm.

As shown in Fig. 2, the core/shell QDs exhibited an excitonic absorption peak at 577 nm and their PL emission peak at 590 nm was red-shifted relative to their absorption peak. The solution molar ratio of Zn^{2+} in the shell to that of ($Zn^{2+} + Cd^{2+}$) in the core was

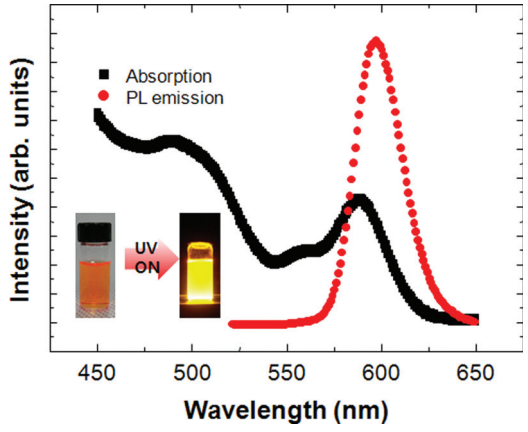

Figure 2. (Color online) UV-visible absorption and PL emission spectra of the core/shell QDs with an absorption peak at 577 nm and an emission peak at 590 nm.

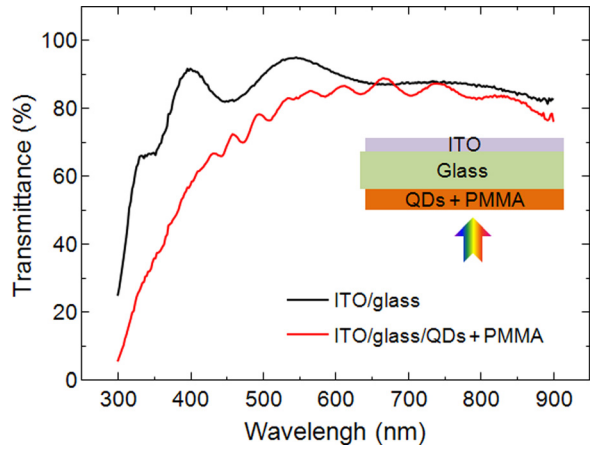

Figure 3. (Color online) The transmittance spectra of the ITO/glass and ITO/glass/QDs + PMMA film. The light is irradiated from the opposite side of the ITO, as shown in the inset figure.

varied and optimized to be 4 to achieve the highest efficiency. The PL quantum yield of the core/shell QDs was measured to be ∼75%, which is higher than (43%) that of the core QDs.

The transmittance values of the ITO/glass and ITO/glass/QDs + PMMA film are shown in Fig. 3. 2 g of PMMA sol was used in this experiment. In all cases, the substrates were illuminated from the opposite side of the ITO, as shown in the inset. In the range from 300 to 600 nm, the transmittance of ITO/glass is higher than that of ITO/glass/QDs + PMMA. The highest transmittance of ITO/glass is measured to be 90% and that of ITO/glass/QDs + PMMA is 85%. In the wavelength range over 600 nm, the transmittance of both samples is similar. It is considered that the lower transmittance of the solar cell employing the QDs + PMMA results in a slightly lower J_{sc} compared to that of the solar cell without the QDs + PMMA film.

Figure 4 shows the typical *J–V* curves of the devices on the bare glass, QDs + 1 g PMMA film coated glass, and QDs + 2 g PMMA film coated glass. In the plot, $V_{oc} = 0.633$ V, $J_{sc} = 9.0$ mA/cm^2, FF = 60.3%, and the power conversion efficiency (PCE) = 3.4% for the device fabricated on bare glass. These values are comparable to the previously reported ones. However, the introduction of the QDs + PMMA film below the glass substrate slightly decreases the response metrics. The device on the QDs + 1 g PMMA film exhibits values of $V_{oc} = 0.633$ V, $J_{sc} = 8.5$ mA/cm^2, FF = 58.6%, and PCE = 3.2%, which are comparable to those of the device on the

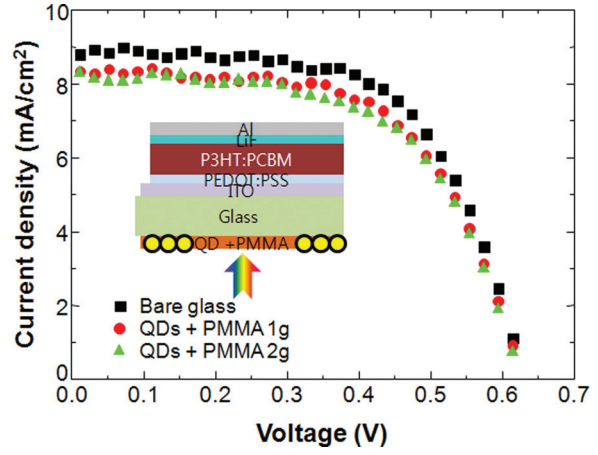

Figure 4. (Color online) *J–V* curves of OPV cell fabricated on bare glass, QDs + 1 g PMMA film coated glass, and QDs + 2 g PMMA film coated glass.

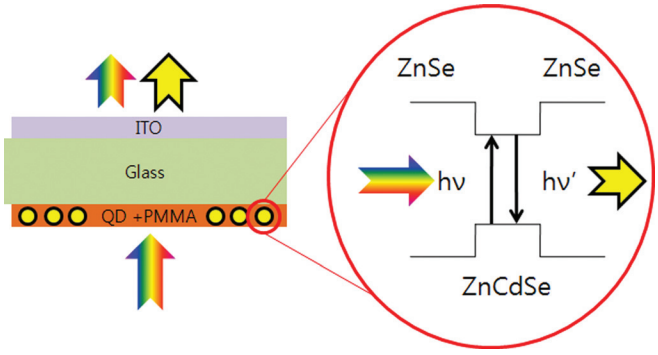

Figure 5. (Color online) Schematic charge transport mechanisms of the OPV cell with QDs + PMMA film.

QDs + 2 g PMMA film fabricated in parallel; for the QDs + 2 g PMMA film, $V_{oc} = 0.613$ V, $J_{sc} = 8.0$ mA/cm^2, FF = 64.0%, and PCE = 3.1%. Compared to the device without the QDs + PMMA film, the device with the QDs + PMMA film showed a slightly lower PCE. As shown in Fig. 3, the transmittance value of ITO on glass with QDs + 2 g PMMA is lower than that of the bare ITO on glass. Therefore, it is thought that the total quantity of light entering into the device with the QDs + PMMA film is lower than that without the QDs + PMMA film, so that the former showed a slightly lower PCE.

Based on these experimental observations, the effect of the ZnCdSe/ZnSe QDs + PMMA film on the properties of the OPV cells can be explained as follows. The absorption spectra of the core/shell QDs showed that the absorption took place in the visible range from 300 to 600 nm. Therefore, the transmittance value of the ITO/glass/QDs + PMMA is lower than that of ITO/glass in the range from 300 to 600 nm, as shown in Fig. 3. This result suggests that the total amount of light absorbed on the P3HT/PCBM active area, which strongly affects PCE, is lower in the OPV cell fabricated on the ITO/glass/QDs + PMMA substrate compared to the device on the ITO/glass substrate. The PL emission range of the QDs was found to be from 570 to 650 nm and the main peak was observed at 590 nm, suggesting that the wavelength of injected light was changed to 570–650 nm, as shown in Fig. 5. It was reported that the absorption range of a P3HT:PCBM = 1:1 sample annealed at 130°C, whose condition is the same as that in this experiment, is from 300 to 700 nm and the main peak is at 520 nm.[15] It seems that the emission range of the QDs overlapped with the absorption range of P3HT:PCBM, but the main peaks did not coincide with each other. This means that the absorption efficiency of P3HT:PCBM with respect to the light emitted from the QDs is not maximized. Therefore, it is thought that the low transmittance of the QDs + PMMA film and the discordance between the main emission peak of the QDs and main absorption peak of P3HT:PCBM induced a slight decrease from 3.4 to 3.2% of the PCE in the OPV cell fabricated on the ITO/glass/QDs + PMMA substrate.

In conclusion, we reported the effect of ZnCdSe/ZnSe core/shell QDs on the efficiency of OPV cells. The V_{oc} of the OPV cell with the QDs + 1 g PMMA film beneath the glass substrate was the same as that of the sample without the QDs, but its J_{sc} and PCE slightly decreased from 9.0 mA/cm^2 and 3.4% to 8.5 mA/cm^2 and 3.2%, respectively. The transmittance value of the ITO/glass sample at a wavelength of 500 nm is 90%, but that of the ITO/glass/QDs + PMMA sample is 80%. The PL spectra showed that the emission range of the QDs was located between 570 and 650 nm, which overlaps with the absorption range of the active area of the OPV cell, P3HT:PCBM. However, the main emission peak of the QDs was observed at 590 nm, which is not coincident with the main absorption peak of P3HT:PCBM (520 nm). Thus, the low transmittance of the QDs + PMMA film and discordance between the emission of the QDs and absorption of P3HT:PCBM induced a slight decrease of the PCE in the OPV cell fabricated on the ITO/glass/QDs + PMMA substrate. It is expected that the usage of QDs whose emission peak is coincident with the absorption peak of the active area in the OPV cells would improve the device properties.

Acknowledgments

This research was supported by Chung-Ang University Research Scholarship Grants in 2010–2011.

References

1. L. G. D. Arco, Y. Zhang, C. W. Schlenker, K. Ryu, M. E. Thompson, and C. Zhou, *ACS Nano*, **4**, 2865 (2010).
2. J. Y. Kim, K. Lee, N. E. Coates, D. Moses, T.-Q. Nguyen, M. Dante, and A. J. Heeger, *Science*, **317**, 222 (2007).
3. G. Zhu, F. Su, T. Lv, L. Pan, and Z. Sun, *Nanoscale Res. Lett.*, **5**, 1749 (2010).
4. W. Lee, J. Lee, S. K. Min, T. Park, W. Yi, and S.-H. Han, *Mater. Sci. Eng., B*, **156**, 48 (2009).
5. K. P. Acharya, T. R. Alabi, N. Schmall, N. N. Hewa-Kasakarage, M. Kirsanova, A. Nemchinov, E. Khon, and M. Zamkov, *J. Phys. Chem. C*, **113**, 19531 (2009).
6. J. Chen, J. L. Song, X. W. Sun, W. Q. Deng, C. Y. Jiang, W. Lei, J. H. Huang, and R. S. Liu, *Appl. Phys. Lett.*, **94**, 153115 (2009).
7. P. Yu, K. Zhu, A. G. Norman, S. Ferrere, A. J. Frank, and A. J. Nozik, *J. Phys. Chem. B*, **110**, 25451 (2006).
8. J. M. Nedeljković, O. I. Mićić, S. P. Ahrenkiel, A. Miedaner, and A. J. Nozik, *J. Am. Chem. Soc.*, **126**, 2632 (2004).
9. D. Deng, M. Shi, F. Chen, L. Chen, X. Jiang, and H. Chen, *Sol. Energy*, **84**, 771 (2010).
10. Y. Zhou, F. S. Riehle, Y. Yuan, H.-F. Schleiermacher, M. Niggemann, G. A. Urban, and M. Krüger, *Appl. Phys. Lett.*, **96**, 013304 (2010).
11. B. R. Saunders and M. L. Turner, *Adv. Colloid Interface Sci.*, **138**, 1 (2008).
12. J. Bang, J. ark, J. H. Lee, N. won, J. Nam, J. Lim, B. Y. Chang, H. J. Lee, B. Chon, J. Shin, J. B. Park, J. H. Choi, K. Cho, S. M. Park, T. Joo, and S. Kim, *Chem. Mater.*, **22**, 233 (2010).
13. L.-W. Chong, H.-T. Chien, and Y.-L. Lee, *J. Power Sources*, **195**, 5109 (2010).
14. P. Reiss, M. Protiere, and L. Li, *Small*, **5**, 154 (2009).
15. V. Shrotriya, J. Ouyang, R. J. Tseng, G. Li, and Y. Yang, *Chem. Phys. Lett.*, **411**, 138 (2005).